

Resonance pressure of electromagnetic radiation on metal nanoparticle

N. I. Grigorchuk

Bogolyubov Institute for Theoretical Physics, National Academy of Sciences of Ukraine,
14-b Metrologichna Street, Kyiv-143, Ukraine, 03143

Received December 03, 2021, in final form February 18, 2022

The influence of the electromagnetic irradiation pressure on a spheroidal metallic nanoparticle at the frequencies close to the surface plasmon vibrations has been considered. With the action of the radiation pressure, the polarizability of metal nanoparticle becomes a tensor quantity. The expressions for the resonance pressure components for the cases of plane-polarized and circularly polarized light have been derived. We have demonstrated that the resonance pressure can substantially depend on the shape of a non-spherical nanoparticle and its orientation with respect to the direction of light propagation and the light polarization.

Key words: *metal nanoparticles, plasmon resonance, pressure of electromagnetic irradiation, light polarization*

1. Introduction

The advent of lasers made the development of researches in the field of microparticle trapping, confinement, and manipulation possible [1]. The hot-electron pressure triggers the anisotropic nanoparticle shape oscillations due to the thermal expansion of the optically heated particles [2]. The resonant radiation pressure on neutral particles was investigated in [3]. Rawson and May observed the angular stabilization of matter by radiation [4] which is familiar to trapping of small particles by radiation pressure. In 1970, Ashkin [5] originally demonstrated, for the first time, the trapping and the manipulation of a micron-sized dielectric spherical particle in the field of two opposing laser beams. Another work [6] was devoted to the observation of resonances in the radiation pressure on dielectric spheres. The plasmon-resonance conditions for optical forces on small particles was then considered in detail by Arias-González and Nieto-Vesperinas [7]. Latter on there was developed a theory of optical tweezers [8]. Much effort to develop the photonic force spectroscopy on metallic nanoparticles was applied by Chaument and coauthors [9].

For the recent years, we have observed an intensive development of the researches of the peculiarities inherent to the mechanisms of light pressure action upon nanoparticles as well as the implication of this action in the tasks of small particle manipulation. Such applications meet a wide usage in biology, medicine, and microelectronics. In the work [10] there was studied the effect of laser induced angular momentum of a spheroidal nanoparticle. The optical radiation force on a dielectric sphere illuminated by a linearly polarized Airy light-sheet was recently studied in [11]. A review of some relevant problems can be found, e.g., in the work [12].

A theoretical study of the time-averaged force exerted upon a spherical particle in a time-harmonic-varying electromagnetic field was carried out in the work [7]. The expression obtained there for the force components depends on the gradient of the electromagnetic wave intensity and on the polarizability of the particle. The particle was considered spherical, so that its polarizability was characterized by a scalar parameter.

In the present work, we consider metallic nanoparticles of the spheroidal form. In this case, the particle polarizability becomes a tensor and can rather strongly depend on the form of the particle [13]. Moreover, the high-frequency (optical) conductivity [14], which is linked to the imaginary part of the particle polarizability and defines its absorption, also becomes a tensor. The dependence of the

polarizability of a metallic nanoparticle on its form becomes especially appreciable in the infra-red range of frequencies. Under such conditions, the expression for the components of the resonance pressure on a nanoparticle with the action of the laser beam, would substantially differ from those obtained in the spherical case.

2. Formulation of the problem

For particles, whose dimensions are considerably smaller than the length of the electromagnetic wave, we apply the Rayleigh approximation, i.e., the particle is considered as a dipole in an uniform field. The force affecting such a particle equals

$$\mathbf{F} = (\mathbf{d} \cdot \nabla) \mathbf{E}^{(0)} + \frac{1}{c} \dot{\mathbf{d}} \times \mathbf{B}^{(0)}, \quad (2.1)$$

where \mathbf{d} is the dipole moment of the particle, $\dot{\mathbf{d}}$ is the time derivative of \mathbf{d} , $\mathbf{E}^{(0)}$ is the electric field and $\mathbf{B}^{(0)}$ is the magnetic field, and c is the speed of light. All quantities in equation (2.1) are real. For our purpose, it is convenient to use the complex quantities, using in equation (2.1) for an arbitrary vector (\mathbf{V}) the symbolic scheme

$$\mathbf{V} \Rightarrow \frac{1}{2}(\mathbf{V} + \mathbf{V}^*). \quad (2.2)$$

We assume that the real and complex conjugate (with asterisk) quantities are varied with time harmonically:

$$\mathbf{V} = \mathbf{V}_0 \exp(-i\omega t), \quad \mathbf{V}^* = \mathbf{V}_0^* \exp(i\omega t). \quad (2.3)$$

Here, ω is the frequency of the electromagnetic wave. The time-dependence of the quantities in (2.3) should determine the rapid oscillations of the force (2.1). Therefore, the special case when this force is averaged over the period T of the wave is of our main interest here.

Let us now introduce the electromagnetic pressure force averaged over this time period:

$$\begin{aligned} \bar{\mathcal{P}} &= \frac{\bar{\mathbf{F}}}{S} = \frac{1}{4T} \int_{-T/2}^{T/2} dt \left\{ [(\mathbf{d} + \mathbf{d}^*) \cdot \nabla] (\mathbf{E} + \mathbf{E}^*) \right. \\ &\quad \left. + \frac{1}{c} (\dot{\mathbf{d}} + \dot{\mathbf{d}}^*) \times (\mathbf{B} + \mathbf{B}^*) \right\}, \end{aligned} \quad (2.4)$$

where the electric \mathbf{E} and magnetic \mathbf{B} fields can be considered as normalized per unit surface area S of the particle. The second term in the integrand of expression (2.4) can be integrated by parts using the well-known Maxwell's equation

$$-\frac{1}{c} \frac{d\mathbf{B}}{dt} = \text{rot } \mathbf{E}. \quad (2.5)$$

Then, instead of equation (2.4), we obtain

$$\begin{aligned} \bar{\mathcal{P}} &= \frac{1}{4T} \int_{-T/2}^{T/2} dt \left\{ [(\mathbf{d} + \mathbf{d}^*) \cdot \nabla] (\mathbf{E} + \mathbf{E}^*) \right. \\ &\quad \left. + (\mathbf{d} + \mathbf{d}^*) \times [\nabla \times (\mathbf{E} + \mathbf{E}^*)] \right\}. \end{aligned} \quad (2.6)$$

Now, taking advantage of the explicit dependence on time [see equations (2.3)], it is easy to carry out the integration in equation (2.6) with respect to the time. The light pressure averaged over the wave period that acts on a dipole with the dipole moment \mathbf{d}_0 in the general case will have the form

$$\begin{aligned} \bar{\mathcal{P}} &= \frac{1}{4} \left\{ (\mathbf{d}_0 \cdot \nabla) \mathbf{E}_0^* + (\mathbf{d}_0^* \cdot \nabla) \mathbf{E}_0 \right. \\ &\quad \left. + \mathbf{d}_0 \times [\nabla \times \mathbf{E}_0^*] + \mathbf{d}_0^* \times [\nabla \times \mathbf{E}_0] \right\}. \end{aligned} \quad (2.7)$$

Later, we will use formula (2.7) to calculate the resonant pressure on a nanoparticle with irradiation by the laser beam.

Herein below, we consider a metallic nanoparticle with an ellipsoid of revolution form. In the reference frame connected to the principal axes of this ellipsoid, the dipole moment of such a particle looks like [15]

$$d_{0j} = \frac{V}{4\pi} \frac{\varepsilon_{jj} - 1}{1 + L_j(\varepsilon_{jj} - 1)} E_{0j}, \quad j = x, y, z. \quad (2.8)$$

Here, V is the volume of the particle, L_j are the depolarization factors,

$$\varepsilon_{jj} = \varepsilon'_{jj} + \varepsilon''_{jj} = \varepsilon' + i \frac{4\pi}{\omega} \sigma_{jj}, \quad (2.9)$$

ε' is the real part of the dielectric constant which has the form

$$\varepsilon' = 1 - \frac{\omega_{pl}^2}{\omega^2}, \quad (2.10)$$

ω_{pl} is the plasma oscillation frequency, and σ_{jj} are the diagonal elements of the tensor of high-frequency (optical) conductivity.

We admit the characteristic dimension of the metallic particle to be smaller than the mean free path of an electron in the direction of its scattering by phonons. Having assumed such a dimension and the asymmetric form of the particle, the conductivity becomes a tensor quantity as it was demonstrated in work [16]. In this case, the conductivity and, therefore, the dissipation are influenced by both the electric field E (electric absorption) and the magnetic field B (magnetic absorption) of the wave. For the case of the ellipsoid of revolution, the following components of the tensor σ_{jj} are distinct from zero in the reference frame connected to the principal axes of this ellipsoid:

$$\sigma_{xx} = \sigma_{yy} \equiv \sigma_{\perp}, \quad \sigma_{zz} \equiv \sigma_{\parallel}, \quad (2.11)$$

while the depolarization factors equal

$$L_x(e_p) = L_y(e_p) = \frac{1}{2} [1 - L_z(e_p)] \equiv L_{\perp}, \quad (2.12)$$

$$L_z(e_p) \equiv L_{\parallel} = \begin{cases} \frac{1-e_p^2}{2e_p^3} \left(\ln \frac{1+e_p}{1-e_p} - 2e_p \right), & R_{\perp} < R_{\parallel}, \\ \frac{1+e_p^2}{e_p^3} (e_p - \arctan e_p), & R_{\perp} > R_{\parallel}. \end{cases} \quad (2.13)$$

In expressions (2.13) the notation

$$e_p^2 = \begin{cases} 1 - R_{\perp}^2/R_{\parallel}^2, & R_{\perp} < R_{\parallel}, \\ R_{\perp}^2/R_{\parallel}^2 - 1, & R_{\perp} > R_{\parallel}, \end{cases} \quad (2.14)$$

is introduced, where R_{\parallel} and R_{\perp} are the corresponding semi-axes of the ellipsoid of revolution.

Introducing the vector components of the dipole moment in the form

$$d_{0i} = \sum_j \alpha_{ij} E_{0j}, \quad (2.15)$$

equations (2.8) and (2.11) yield the following expressions for nonzero components of the polarizability tensor α_{jj} :

$$\alpha_{xx} = \alpha_{yy} \equiv \alpha_{\perp} = \frac{V}{4\pi} \frac{(\varepsilon_{\perp} - 1)}{1 + L_{\perp}(\varepsilon_{\perp} - 1)}, \quad (2.16)$$

$$\alpha_{zz} \equiv \alpha_{\parallel} = \frac{V}{4\pi} \frac{(\varepsilon_{\parallel} - 1)}{1 + L_{\parallel}(\varepsilon_{\parallel} - 1)}, \quad (2.17)$$

where

$$\varepsilon_{\parallel} = \varepsilon' + i \frac{4\pi}{\omega} \sigma_{\parallel}, \quad \varepsilon_{\perp} = \varepsilon' + i \frac{4\pi}{\omega} \sigma_{\perp}. \quad (2.18)$$

The expressions for σ_{\perp} and σ_{\parallel} under various specific conditions are presented in work [13]. In particular, if the electric absorption dominates, simple analytical expressions for the components σ_{\perp} and σ_{\parallel} can be obtained in the cases of strongly prolate ($R_{\parallel} \gg R_{\perp}$) and strongly oblate ($R_{\parallel} \ll R_{\perp}$) ellipsoids [13]:

$$\sigma_{\parallel} \approx \frac{3}{2} \sigma_{\perp} \approx \frac{9\pi}{64} \frac{v_F}{R_{\perp}} \frac{ne^2}{m\omega^2}, \quad (R_{\parallel} \gg R_{\perp}), \quad (2.19)$$

$$\sigma_{\parallel} \approx \frac{1}{2} \sigma_{\perp} \approx \frac{9}{16} \frac{v_F}{R_{\parallel}} \frac{ne^2}{m\omega^2}, \quad (R_{\parallel} \ll R_{\perp}). \quad (2.20)$$

Here, v_F is the Fermi velocity, n is the concentration of electrons, and m is the electron mass.

For spherical particles ($R_{\parallel} = R_{\perp} = R$), we obtain

$$\sigma_{\parallel} = \sigma_{\perp} = \frac{3}{4} \frac{v_F}{R} \frac{ne^2}{m\omega^2}. \quad (2.21)$$

Formulae (2.19) and (2.20) are valid in the case of high-frequency fields, when the frequency of light is higher than the transit-time frequencies ($\omega > v_F/R_{\perp}, v_F/R_{\parallel}$).

Starting from formula (2.15) using equation (2.11), the dipole moment can be written down for an arbitrary coordinate system in the form

$$\mathbf{d}_0 = \alpha_{\perp} \mathbf{E}_0 - (\alpha_{\perp} - \alpha_{\parallel}) (\mathbf{n} \mathbf{E}_0) \mathbf{n}. \quad (2.22)$$

Here, \mathbf{n} is a unit vector directed along the axis of revolution of the ellipsoid. Formulae (2.22) and (2.7) will serve as the basic ones for studying the light pressure on a nanoparticle.

3. Pressure caused by the action of an electromagnetic wave

In order to obtain an explicit expression for the time-averaged pressure (2.7), it is necessary to establish the coordinate dependence of the field \mathbf{E}_0 . As the first example of such a dependence, we take this field having a linear polarization along x -axis. It looks as follows:

$$\mathbf{E}_0 = (E_x, 0, 0), \quad E_x = E_0 e^{-x^2/(2a^2)} e^{ikz}, \quad (3.1)$$

where a is the radius of the light beam. Substituting expressions (2.22) and (3.1) into equations (2.7), we obtain the expressions for nonzero components of the time-averaged particle pressure:

$$\overline{\mathcal{P}}_x = -\frac{x}{2a^2} \left[|E_0|^2 \operatorname{Re} \alpha_{\perp} + |\mathbf{E}_0 \mathbf{n}|^2 \operatorname{Re} (\alpha_{\parallel} - \alpha_{\perp}) \right], \quad (3.2)$$

$$\overline{\mathcal{P}}_z = \frac{k}{2} \left[|E_0|^2 \operatorname{Im} \alpha_{\perp} + |\mathbf{E}_0 \mathbf{n}|^2 \operatorname{Im} (\alpha_{\parallel} - \alpha_{\perp}) \right], \quad (3.3)$$

where \mathbf{E}_0^2 is the energy density of electromagnetic field. For the linear field polarization along y -axis, one must change in equation (3.2) x by y .

The real and imaginary parts of the polarizability tensor can be written as [16]

$$\operatorname{Re} \alpha_{(\parallel)} = \frac{V}{4\pi L_{(\parallel)}} \frac{\left[(1 - \xi_m) \omega^2 - \omega_{(\parallel)}^2 \right] \left[\omega^2 - \omega_{(\parallel)}^2 \right] + \left[2\omega\gamma_{(\parallel)} \right]^2}{\left[\omega^2 - \omega_{(\parallel)}^2 \right]^2 + \left[2\omega\gamma_{(\parallel)} \right]^2}, \quad (3.4)$$

and

$$\text{Im } \alpha_{(\perp)} = \frac{V}{4\pi L_{(\perp)}} \frac{2\omega^3 \xi_m \gamma_{(\perp)}}{\left[\omega^2 - \omega_{(\perp)}^2 \right]^2 + \left[2\omega \gamma_{(\perp)} \right]^2}, \quad (3.5)$$

where we have introduced the notations

$$V = \frac{4}{3}\pi R_{\parallel} R_{\perp}^2, \quad (3.6)$$

$$\xi_m = \frac{\epsilon_m}{\epsilon_m + L_{(\perp)} - L_{(\parallel)} \epsilon_m}, \quad (3.7)$$

$$\omega_{(\perp)}^2 = \frac{L_{(\perp)}}{\epsilon_m + L_{(\perp)} - L_{(\parallel)} \epsilon_m} \omega_{\text{pl}}^2, \quad (3.8)$$

and

$$\gamma_{(\perp)} \equiv \gamma_{(\perp)}(\omega) = \frac{2\pi L_{(\perp)}}{\epsilon_m + L_{(\perp)} - L_{(\parallel)} \epsilon_m} \sigma_{(\perp)}(\omega) \quad (3.9)$$

represents the half-width of the resonance curve for the light polarized along (\parallel) or across (\perp) the revolution axis of the spheroid; ϵ_m is the dielectric constant of the medium.

For the particle of a spherical form emersed in the medium with $\epsilon_m = 1$, in the field of the same wave, one gets

$$\overline{\mathcal{P}}_{z, \text{sph}} = \frac{k}{2} e^{-x^2/a^2} E_0^2 \text{Im } \alpha_{\text{sph}}, \quad (3.10)$$

$$\overline{\mathcal{P}}_{i, \text{sph}} = -\frac{x_i}{2a^2} e^{-x^2/a^2} E_0^2 \text{Re } \alpha_{\text{sph}}, \quad (3.11)$$

where $x_i = x, y$ and

$$\text{Re } \alpha_{\text{sph}} = R^3 \frac{(\epsilon' - 1)(\epsilon' + 2) + (4\pi\sigma/\omega)^2}{(\epsilon' + 2)^2 + (4\pi\sigma/\omega)^2}, \quad (3.12)$$

$$\text{Im } \alpha_{\text{sph}} = R^3 \frac{12\pi\sigma/\omega}{(\epsilon' + 2)^2 + (4\pi\sigma/\omega)^2}, \quad (3.13)$$

$$\sigma = \frac{3}{16\pi} \frac{v_F}{R} \left(\frac{\omega_{\text{pl}}}{\omega} \right)^2. \quad (3.14)$$

Here, R is the radius of a spherical particle, σ is its high-frequency optical conductivity, and we take into account equation (2.10). Expressions (3.4) and (3.5), obtained for spheroidal particles, clearly transforms into the corresponding expressions (3.12) and (3.13) for spherical particles with the account of the equality $L_{\parallel} = L_{\perp} = 1/3$. Then, the conductivity becomes a scalar quantity, specified in the form (3.14). At the plasma frequency, the real part of the permittivity tends to zero.

Consider now the elliptical polarized Gaussian beam:

$$\mathbf{E}_0 = (\mathbf{b}_1 + i\mathbf{b}_2) e^{-(x^2+y^2)/2a^2} e^{ikz}, \quad (3.15)$$

$$\mathbf{b}_1 = (b_1, 0, 0), \quad \mathbf{b}_2 = (0, b_2, 0). \quad (3.16)$$

In this case, after substituting equations (3.15), (3.16), and (2.22) into equation (2.7), we obtain

$$\begin{aligned} \overline{\mathcal{P}}_i &= -\frac{x}{2a^2} e^{-(x^2+y^2)/a^2} \left\{ (b_1^2 + b_2^2) \text{Re } \alpha_{\perp} \right. \\ &\quad \left. + [(\mathbf{n} \mathbf{b}_1)^2 + (\mathbf{n} \mathbf{b}_2)^2] \text{Re } (\alpha_{\parallel} - \alpha_{\perp}) \right\}, \end{aligned} \quad (3.17)$$

with $i = x, y$,

$$\begin{aligned} \overline{\mathcal{P}}_z &= \frac{k}{2} e^{-(x^2+y^2)/a^2} \{ (b_1^2 + b_2^2) \text{Im } \alpha_{\perp} \\ &+ [(\mathbf{n} \mathbf{b}_1)^2 + (\mathbf{n} \mathbf{b}_2)^2] \text{Im} (\alpha_{\parallel} - \alpha_{\perp}) \}. \end{aligned} \quad (3.18)$$

One should bear in mind that \mathbf{n} is a unit vector directed along the revolution axis of the ellipsoid. We see that in this case, the light pressure depends on two angles — between vectors \mathbf{n} and \mathbf{b}_1 and between \mathbf{n} and \mathbf{b}_2 vectors.

If the components of the unit vector, appearing in equation (2.22), in a spherical coordinate system are represented as

$$n_x = \sin \theta \cos \varphi, \quad n_y = \sin \theta \sin \varphi, \quad n_z = \cos \theta, \quad (3.19)$$

then the products $\mathbf{n} \mathbf{b}_1$ and $\mathbf{n} \mathbf{b}_2$ in equations (3.17) and (3.18), respectively, become

$$\mathbf{n} \mathbf{b}_1 = b_1 \sin \theta \cos \varphi, \quad \mathbf{n} \mathbf{b}_2 = b_2 \sin \theta \sin \varphi. \quad (3.20)$$

In this case, the ratio of the average values of the light pressure on a metal particle, having spheroidal and spherical forms in the direction of incidence of the radiation can be written, using equations (3.18) and (3.10), as follows

$$\frac{\overline{\mathcal{P}}_z}{\overline{\mathcal{P}}_z|_{\text{sph}}} = \frac{\text{Im } \alpha_{\perp}}{\text{Im } \alpha_{\text{sph}}} + \sin^2 \theta \frac{(b_1 \cos \varphi)^2 + (b_2 \sin \varphi)^2}{b_1^2 + b_2^2} \frac{\text{Im} (\alpha_{\parallel} - \alpha_{\perp})}{\text{Im } \alpha_{\text{sph}}}. \quad (3.21)$$

From equation (3.21), one can see that, contrary to the particles having a spherical form (when $\alpha_{\perp} = \alpha_{\parallel}$), the light pressure components for the nanoparticles with the ellipsoid of revolution geometry acquire the dependence on the angle between the field direction and the revolution axis of the ellipsoid. In addition, these components depend on the particle's form itself, which is determined by the depolarization factors L_j included in the diagonal components of the tensor α_{jj} . An analogous relation one can also obtain for the ratio of the conservative pressure components P_i if the imaginary parts of α in equation (3.21) are replaced by their real parts.

In the case of circular polarization, $\mathbf{b}_1 = \mathbf{b}_2 = \mathbf{b}$, so that

$$(\mathbf{n} \mathbf{b}_1)^2 + (\mathbf{n} \mathbf{b}_2)^2 = (n_x^2 + n_y^2) b^2 = (1 - n_z^2) b^2. \quad (3.22)$$

That is, in this case, only the dependence on the angle between the vector \mathbf{n} and the direction of the beam propagation survives.

Thus, similarly to the cases of plane-polarized and circularly polarized light beams, the time-averaged light pressure that tests a non-spherical metallic nanoparticle becomes angle-dependent. In addition, this pressure depends on the particle's form through the components α_{\perp} and α_{\parallel} of the polarization tensor; this dependence manifests itself to the maximal extent in the infra-red range of the spectrum (in the vicinity of the CO₂-laser frequency). For example, taking $\omega_{\text{pl}} \approx 8 \cdot 10^{15} \text{ s}^{-1}$ for gold and $\omega = 2 \cdot 10^{14} \text{ s}^{-1}$ for the CO₂-laser frequency, we obtain $\varepsilon' \approx -1600$. Therefore, the combinations $L_{\perp, \parallel} (\varepsilon_{\perp, \parallel} - 1)$ that enter the denominators of formula (2.16) or (2.17) will be approximately equal

$$L_{\perp, \parallel} (\varepsilon_{\perp, \parallel} - 1) \approx -1600 L_{\perp, \parallel}. \quad (3.23)$$

Since the quantities L_{\parallel} and L_{\perp} may vary from 0 to 1 (provided that $2L_{\perp} + L_{\parallel} = 1$), it is clear to what extent the quantity (3.2) and, respectively, the quantities α_{\perp} and α_{\parallel} can be sensitive to the form of a metallic particle within this range of frequencies.

4. Light pressure at plasmon resonance

From equations (3.4) and (3.5) it is easy to determine the real and imaginary parts of $\alpha_{\parallel, \perp}$ at resonance frequencies

$$\text{Re } \alpha_{\parallel, \perp} = \frac{V}{4\pi L_{\parallel, \perp}}, \quad \text{Im } \alpha_{\parallel, \perp} = \frac{V}{(4\pi L_{\parallel, \perp})^2} \frac{\omega_{\parallel, \perp}}{\sigma_{\parallel, \perp}}. \quad (4.1)$$

For a specified frequency, one can always choose a geometric form of the particle such that it will experience a resonant increase of the absorption with electromagnetic light pressure. In particular, for particles of spheroidal shape, there exist two forms of the spheroid which can resonantly absorb radiation. The converse is also true: a nanoparticle of an arbitrary geometric shape will absorb resonantly at least one frequency. The higher is the degree of symmetry of the particle, the smaller is the number of resonant frequencies that it can absorb. For example, a spherical particle has one resonant frequency, a spheroidal particle has got two, and an ellipsoidal particle three.

As one can see from equation (3.21), the value of the ratio of light pressures on a metallic particle depends both on the angle of light incidence θ and on the light polarization angle φ . Studies have shown that this ratio reaches a maximum value at the angle of incidence equal to $\theta = \pi/2$. Setting the angle in equation (3.21) equal to $\theta = \pi/2$, let us investigate here how this relation changes for different polarizations of the incident Gaussian beam with a change in the shape of the nanoparticle. As an example, select the Cu nanoparticle.

Figure 1 illustrates the ratio of the light pressure on spheroidal Cu nanoparticle to the light pressure on spherical Cu nanoparticle in the direction of incidence of the laser beam, as a function of the deviation of the shape of the particle from the spherical one. The frequency of laser beam was chosen as $\omega = 2.9 \cdot 10^{15} \text{ s}^{-1}$, which is close to the plasmon modes in copper and $\epsilon_m = 1$. As one can see, the resonant light pressure at that frequency is experienced by particles close to spherical shape. Figure 2 shows the same dependence for the laterally directed forces. Here and below, the force calculations are done using equation (3.21) and the analogous expression obtained with the replacement $\text{Im} \rightarrow \text{Re}$ for the i -th pressure. As is seen in figure 1, the light pressure on the Cu particle at the plasmon resonance in the direction of incidence of the laser beam can be hundreds of times greater than the pressure experienced by a spherical particle of an equal volume.

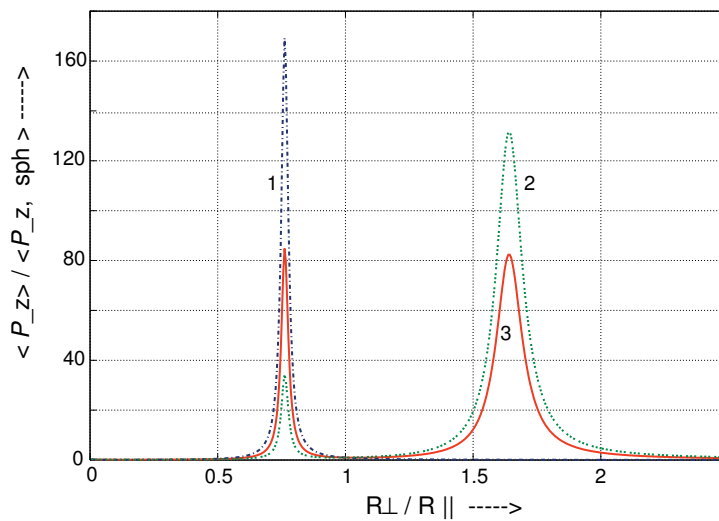


Figure 1. (Colour online) The ratio of the light pressure on spheroidal Cu nanoparticle to the pressure on spherical Cu nanoparticle of an equal volume with the radius of 100 Å, as a function of the Cu shape, in the direction of the action of the laser beam with frequency $\omega \simeq 2.9 \cdot 10^{15} \text{ s}^{-1}$ for the different polarization: curve 1 (short-dashed line) corresponds to the linear polarization; curve 2 (long-dashed line) corresponds to the elliptical polarization with $b_1/b_2 = 1/2$; curve 3 (solid line) corresponds to the circular polarization.

In the lateral directions (figure 2), this factor is considerably smaller, not exceeding ten times. In this case, the light pressures ratio has both positive and negative value that speaks for the attractive or repulsive nature of the force (the “radiation wind”) acting on a nanoparticle in this direction. It reaches the maximum in absolute value at the angle $\varphi = \pi/2$.

With an increasing frequency of the incident radiation, the plasmon resonance occurs in prolate nanoparticles with a greater ratio of R_{\perp}/R_{\parallel} , while for oblate nanoparticles it occurs with smaller values of R_{\perp}/R_{\parallel} . In the last case, the pressure forces on the nanoparticle fall off in absolute value.

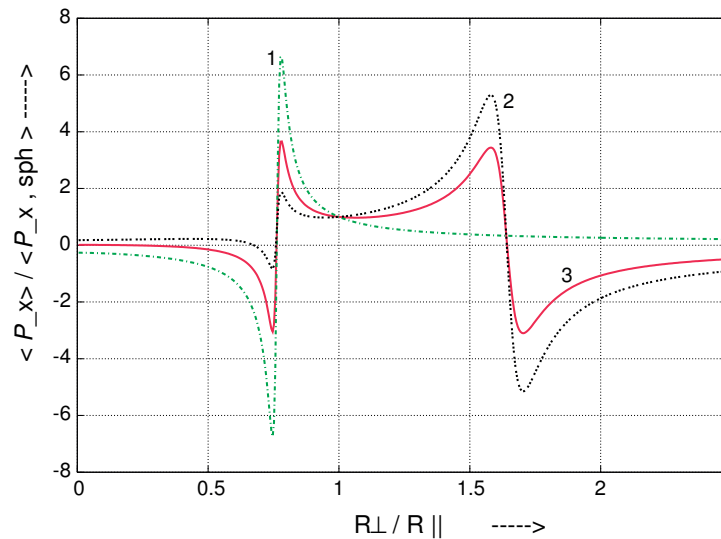


Figure 2. (Colour online) The same as in figure 1 for the lateral x -direction of the action of the laser beam.

It is also seen (figure 2) that together with the resonance for prolate particles there is also a resonance for oblate particles in the lateral directions, and for low degrees of oblateness this resonance is not suppressed by attenuation as it would be the case at CO_2 -laser frequency. In the direction of incidence of the radiation along the z axis (figure 1), the resonances appear in the form of peaks lying on each side from the spherical shape $R_{\perp}/R_{\parallel}=1$.

At the pointed above plasmon frequency for Cu, the resonance light pressure will be manifest itself [in accordance with equations (3.8) and (2.13)] for both prolate and oblate nanoparticles with the following values of the ratio $R_{\perp}/R_{\parallel} = 0.763$, and $R_{\perp}/R_{\parallel} = 1.64$, respectively. Consequently, the left-hand peak (figure 1) and resonance (figure 2) pertain to the prolate metal particle, while the right-hand peak and resonance belong to the oblate metal particle.

With a decrease in the angle of fall θ (with a fixed angle φ), the peak and resonance for the prolate Cu nanoparticle are suppressed, whereas for the oblate Cu nanoparticle they reach maximum values. For a specified orientation (i.e., fixed θ), the enhancement or suppression of the peaks and resonances in Cu nanoparticles of different shape can be reached by a suitable choice of polarization of the incident radiation [17].

With a change in the shape of the nanoparticle there occurs a shift of the plasmon peaks of the light pressure. To elucidate the nature of these shifts with the change in the degree of oblateness or prolateness of the Cu nanoparticle, in figure 3 we have plotted the frequency dependence for the ratio of the light pressure on nanoparticles with different shapes at fixed angles. The weak peaks 3 and 4 in this figure pertain to the Cu nanoparticles which are close to spherical in shape.

As can be seen from figure 3, the oblate nanoparticles manifest a resonant light pressure at longer wavelengths (curves 1, 2) in comparison with a spherical metallic nanoparticle, and the prolate nanoparticles manifest it at shorter wavelengths (curves 5, 6). Here, the tails of the peaks of the oblate nanoparticles extend toward the long-wavelength side of the spectrum, while those of the prolate nanoparticles extend toward the short-wavelength side. As the flatness of the nanoparticle increases (curve 1), the resonance pressure peak on a nanoparticle increases in absolute value and shifts to the longer wavelengths, while with an increasing elongation of the nanoparticle (curve 6) there is, in addition to an increase of its pressure, the shift of the peak to the shorter wavelengths of the spectrum takes place.

The peaks labeled by numbers with a prime in figure 3 arise together with the peaks labeled with the corresponding unprimed numbers; as is seen from equation (3.7), this is due to the fact that they fall into the established spectrum of R_{\perp}/R_{\parallel} values. Their intensity depends on two factors: the orientation of the particle with respect to the incident radiation and/or polarization of the radiation. In the given example, the height of the primed peaks can be controlled by means of the angle θ ; they vanish for $\theta \rightarrow 0$.

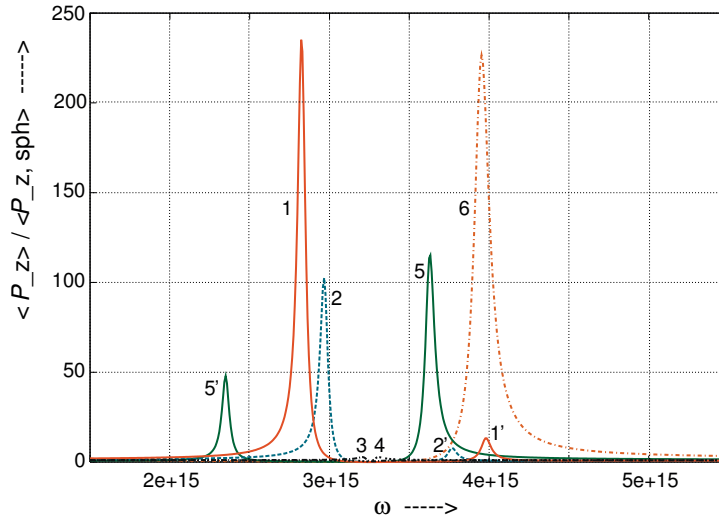


Figure 3. (Colour online) Frequency dependence of the ratio of light pressure on Cu nanoparticle with a spheroidal shape and the light pressure on the spherical Cu nanoparticle of an equal volume in the direction of incident laser beam for nanoparticles with the radius of 100 Å and different R_{\perp}/R_{\parallel} : 1.8 (1), 1.5 (2), 1.05 (3), 0.95 (4) 0.5 (5) 0.1 (6); for angles $\varphi = \pi/4$, $\theta = \pi/12$. $\epsilon_m = 1$.

It should be noted that for prolate nanoparticles, the growth of the intensity and the shift of the peak tend to saturation with an increasing prolateness of the nanoparticle, after which a further increase of the prolateness leads to a fall-off of the values of the light pressure on a nanoparticle and the shift of the peak does not occur. Estimates show that for $R_{\perp}/R_{\parallel} = 1/64$, the peak has already become rather wide, and its shift is not very noticeable in comparison with that for $R_{\perp}/R_{\parallel} = 1/32$, for example.

5. Discussions

We have considered the radiation pressure on a very small (Rayleigh) metal particle when the dipole approximation can be applied. The effects of resonant radiation pressure on neutral nanoparticles were studied previously by Gómez-Medina with coauthors [3]. They showed that a small particle in a hollow waveguide can be strongly accelerated along the guide axis while being highly confined in a narrow zone of the cross section of the guide. In the general case, whether a neutral nanoparticle will be attracted to or pushed away from the high-intensity region of the laser field and accelerated depends on the ratio of the components of the gradient and scattering-absorbing forces [7].

In section 3 it was implicitly assumed that the metallic nanoparticle is placed at the center of the beam. If one considers the deviation of metallic nanoparticle placement from the center of the beam, then, depending on the ratio of the pressure force to the mass of the particle, one should most likely expect one of the two scenarios: either its revolution ([10]) around an axis passing through the center of mass, or acceleration in the direction of the beam.

6. Conclusion

We have obtained analytical expressions for the force of resonance pressure on a spheroidal metallic nanoparticle which is exerted by a laser beam averaged over a period of the incident wave. It is shown that the pressure components can substantially depend on the shape of the particle as well as on the angles that define its orientation both relative to the direction of the incident radiation and relative to the polarization of the beam.

We have investigated the behavior of the electromagnetic pressure force on a nanoparticle near plasmon resonances in spheroidal nanoparticles in relation to the shape and orientation of the nanoparticle. We

have found the shift of the resonance peak of the pressure towards longer wavelengths for more oblate metallic nanoparticles and towards shorter wavelengths for more prolate ones. We have established that the value of the light pressure with the laser beam action on spheroidal metallic nanoparticle can differ by orders of magnitude from the analogous light pressure acting on a spherical metallic particle of the same volume.

Acknowledgements

Author is grateful to the Program of the Fundamental Research of the Department of Physics and Astronomy of the National Academy of Sciences of Ukraine (NASU) (0121U109816) for financial support of this work.

References

1. Iida T., Ishihara H., *Phys. Rev. Lett.*, 2003, **90**, 057403, doi:10.1103/PhysRevLett.90.057403.
2. Perner M., Gresillon S., März J., von Plessen G., Feldmann J., Porstendorfer J., Berg K.-J., Berg G., *Phys. Rev. Lett.*, 2000, **85**, 792–795, doi:10.1103/PhysRevLett.85.792.
3. Gómez-Medina R., San José P., García-Martín A., Lester M., Nieto-Vesperinas M., Sáenz J. J., *Phys. Rev. Lett.*, 2001, **86**, 4275–4278, doi:10.1103/PhysRevLett.86.4275.
4. Rawson E. G., May A. D., *Appl. Phys. Lett.*, 1966, **8**, 93–96, doi:10.1063/1.1754503.
5. Ashkin A., *Phys. Rev. Lett.*, 1970, **24**, 156–159, doi:10.1103/PhysRevLett.24.156.
6. Ashkin A., Dziedzic J. M., *Phys. Rev. Lett.*, 1977, **38**, 1351–1354, doi:10.1103/PhysRevLett.38.1351.
7. Arias-González J. R., Nieto-Vesperinas M., *J. Opt. Soc. Am. A*, 2003, **20**, 1201–1209, doi:10.1364/JOSAA.20.001201.
8. Novotny L., Bian R. X., Xie X. S., *Phys. Rev. Lett.*, 1997, **79**, 645–648, doi:10.1103/PhysRevLett.79.645.
9. Chaumet P. C., Rahmani A., Nieto-Vesperinas M., *Phys. Rev. B*, 2005, **71**, 045425, doi:10.1103/PhysRevB.71.045425.
10. Grigorchuk N. I., *J. Opt. Soc. Am. B*, 2018, **35**, 2851–2858, doi:10.1364/JOSAB.35.002851.
11. Song N., Li R., Sun H., Zhang J., Wei B., Zhang S., Mitri F. G., *J. Quant. Spectrosc. Radiat. Transfer*, 2020, **245**, 106853, doi:10.1016/j.jqsrt.2020.106853.
12. Sukhov S., Dogariu A., *Rep. Prog. Phys.*, 2017, **80**, 112001, doi:10.1088/1361-6633/aa834e.
13. Tomchuk P. M., Grigorchuk N. I., *Phys. Rev. B*, 2006, **73**, 155423, doi:10.1103/PhysRevB.73.155423.
14. Grigorchuk N. I., *Europhys. Lett.*, 2018, **121**, 67003, doi:10.1209/0295-5075/121/67003.
15. Bohren C. F., Huffman D. R., *Absorption and Scattering of Light by Small Particles*, Wiley, Weinheim, 2004.
16. Grigorchuk N. I., *Europhys. Lett.*, 2012, **97**, 45001, doi:10.1209/0295-5075/97/45001.
17. Kimura H., Mann I., *J. Quant. Spectrosc. Radiat. Transfer*, 1998, **60**, 425–438, doi:10.1016/S0022-4073(98)00017-X.

Резонансний тиск електромагнітного випромінювання на металеву частинку

М. І. Григорчук

Інститут теоретичної фізики ім. М. М. Боголюбова НАН України, вул. Метрологічна, 14-Б, Київ-143, Україна, 03143

Розглянуто вплив тиску електромагнітного випромінювання на сферічну металеву частинку на частотах, близьких до частот коливань поверхневого плазмона. Під тиском випромінювання поляризованість металеві наночастинки стає тензорною величиною. Одержані вирази для компонент резонансного тиску для випадків плоско-поляризованого та циркулярно-поляризованого світла. Показано, що резонансний тиск може істотно залежати від форми несферичної частинки та від її орієнтації стосовно напрямку поширення світла і його поляризації.

Ключові слова: металеві наночастинки, плазмонний резонанс, тиск електромагнітного випромінювання, поляризація світла
